

# An Iterative Substructuring Method for Coupled Fluid-Solid Acoustic Problems

Jan Mandel

*Department of Mathematics and Center for Computational Mathematics, University of Colorado at Denver, Denver, CO 80217-3364, U.S.A., and Department of Aerospace Engineering Science and Center for Aerospace Structures, University of Colorado at Boulder, Boulder, CO 80309-0429, U.S.A*

November 2000

Revised December 2001

Accepted for publication in  
Journal of Computational Physics  
as of January 17, 2002

---

A fast parallel iterative method is proposed for the solution of linear equations arising from Finite Element discretization of the time harmonic coupled fluid-solid systems in fluid pressure and solid displacement formulation. The fluid and the solid domains are decomposed into non-overlapping subdomains. Continuity of the solution is enforced by Lagrange multipliers. The system is augmented by duplicating the degrees of freedom on the wet interface. The original degrees of freedom are then eliminated and the resulting system is solved by iterations preconditioned by a coarse space correction. In each iteration, the method requires the solution of one independent local acoustic problem per subdomain and the solution of a global problem with several degrees of freedom per subdomain. Computational results show that the method is scalable with the problem size, frequency, and the number of subdomains. The method generalizes the FETI-H method for the Helmholtz equation to coupled fluid-elastic scattering. The number of iterations is about same as for the FETI-H method for the related Helmholtz problem with Neumann boundary condition instead of an elastic scatterer if enough coarse space functions are used. Convergence behavior is explained from the spectrum of the iteration operator and from numerical near decoupling of the equations in the fluid and in the solid regions.

---

*Key Words:* Lagrange multipliers, domain decomposition, iterative substructuring, elastic scattering, Helmholtz equation, coupled fluid-solid acoustics, FETI

## 1. INTRODUCTION

In this paper, a new iterative substructuring method is proposed for the solution of the coupled fluid-elastic time harmonic scattering problem. Iterative solution of the coupled problem by alternating between the fluid and the elastic problem is known, cf., Achil'diev and Nazhmidinov [1] or Cummings and Feng [2]. The new method extends the FETI-H domain decomposition method, proposed by De La Bourdonnaye et al. [3] and Farhat et al. [4, 5] for the solution of the Helmholtz equation, to an iterative method for the coupled problem.

The new method for the coupled problem is designed so that the interaction between the fluid and the solid is resolved at the same time as the solution within the fluid and the elastic domains, and the fluid part of the iteration operator reduces to the operator in FETI-H in the limit when the scatterer becomes rigid. The method also uses the same basic building blocks in the fluid subdomain as FETI-H, making software reuse easier.

The FETI method was originally proposed by Farhat and Roux [6] for solving linearized elasticity problems. The basic idea of all FETI-type methods is to decompose the domain into non-overlapping subdomains and to use Lagrange multipliers to enforce that the values of the degrees of freedom coincide on the interfaces between the subdomains. The original degrees of freedom are then eliminated, leaving a dual system for the Lagrange multipliers, which is solved iteratively. To achieve scalability with the number of subdomains, a coarse problem is required. For elasticity, the coarse problem formed naturally from nullspaces of the local subdomain matrices results in a scalable method, cf., Farhat et al. [7] and Mandel and Tezaur [8]. The general coarse problem in FETI was introduced by Farhat and Mandel [9, 10]; this is the approach used in FETI-H and in the present method, with plane waves as the generators of the coarse problem. For further information on FETI, see [11, 12, 13, 14, 15] and references therein. The modifications of the FETI method for the Helmholtz equation involve replacing the conditions for the continuity of the solution and its normal derivatives on subdomain interfaces by their complex linear combination to obtain a radiation condition, inspired by Després [16]. The present modification of FETI for elastic scattering uses a complex linear combination of continuity conditions for the displacement and the traction, related to a method by Bennethum and Feng [17].

Related variants of the FETI method for the Helmholtz equation of scattering were proposed by De La Bourdonnaye et al. [3], Farhat et al. [18], and Tezaur et al. [19]. For other work on iterative methods for indefinite problems arising from scattering, see, e.g., [20, 21, 22, 23, 24].

The distinctive feature of the present method is the treatment of the wet interface. The fluid region and the elastic region are divided into nonoverlapping subdomains. The division into subdomains does not need to match across the wet interface. This comes naturally because, due to the selection of the variational form of the problem, the wet interface conditions are enforced only weakly. The degrees of freedom on the wet interface are duplicated and new equations are added to enforce the equality of the duplicates. The original degrees of freedom in all subdomains are then eliminated. The intersubdomain Lagrange multipliers and the duplicates of the degrees of freedom on the wet interface are retained and form the reduced problem,

which is solved iteratively. The diagonal blocks for the intersubdomain Lagrange multipliers in the reduced problems are exactly same as in the FETI-H method and its straightforward extension to elasticity. There are no Lagrange multipliers across the wet interface. Instead, the fluid and the elastic region communicate by way of the duplicated primal variables on the wet interface only. This primal-dual approach is reminiscent of the Dual-Primal FETI method (FETI-DP) for positive definite problems [25, 26].

Another important feature of the present method is scaling. While scaling of different physical fields is routine, here we benefit from the fact that as the stiffness of the scatterer approaches infinity, the fluid and elastic parts of the discretized coupled problem become uncoupled in the limit.

The coarse space of FETI-H consists of plane waves for the Lagrange multipliers between the fluid subdomains. The present method includes also plane waves for the multipliers on interfaces between the elastic regions, and for the primal variables on the wet interface. When the same number of coarse functions are used in each of the two added categories as for FETI-H, the number of iterations is similar to the iteration count for the FETI-H method for the same problem with a rigid scatterer.

The present formulation of the method is for bounded regions only. While the formulation of the method is dimension independent, numerical results are given only for a prototype implementation in 2D. Performance in 3D, further development of the method, theoretical analysis, and parallel implementation will be reported elsewhere.

The paper is organized as follows. Section 2 introduces the notation. In Section 3, we review the FETI-H method as a starting point. In Section 4, a straightforward extension is proposed for scattering in an elastic medium. The new method for the coupled fluid-elastic problem is presented in Section 5. Explanations of the convergence properties of the method are given in Section 6. Implementation details are discussed in Section 7. Complexity of the algorithm is addressed in Section 8. Section 9 contains computational results, and Section 10 is the conclusion.

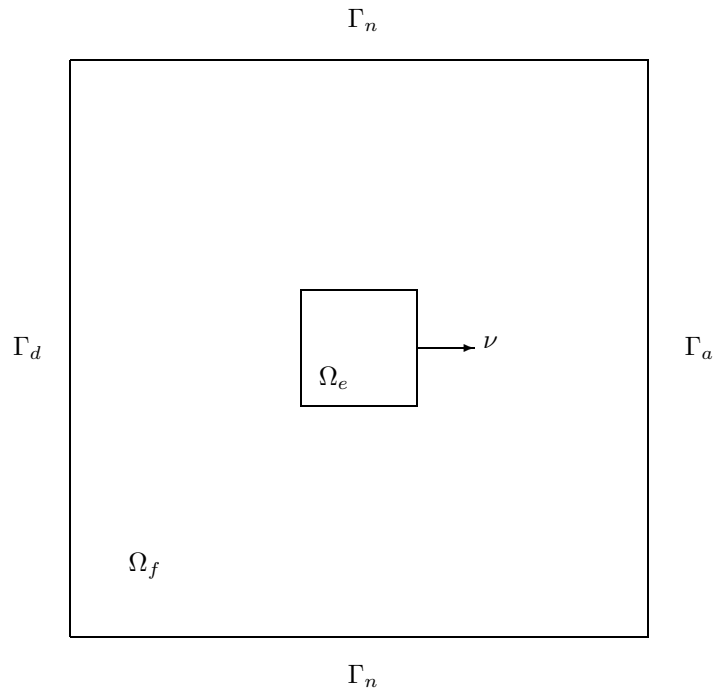
## 2. NOTATION

The space  $H^1(\Omega)$  is the Sobolev space of functions with square integrable first order generalized derivatives. Functions are denoted by  $p, u$ , etc. The corresponding vectors of values of degrees of freedom are  $\mathbf{p}, \mathbf{u}$ . Matrices are denoted by  $\mathbf{A}, \mathbf{B}, \dots$ . The symbol  $T$  denotes the transpose. Quantities associated with subdomain  $\Omega^s$  are denoted by superscript  $s$ , e.g.,  $p^s, \mathbf{p}^s$ . Block vectors or matrices where each block consists of subdomain vectors or matrices are denoted as  $\hat{\mathbf{u}}, \hat{\mathbf{A}}$ , and after scaling, as  $\tilde{u}, \tilde{A}$ . The external normal vector is denoted by  $\nu$ . The symbol  $\approx$  means ‘‘approximately equal’’ and  $\ll$  means ‘‘much less than’’. Finally,  $\|\mathbf{f}\|$  is the  $\ell^2$  norm and of a vector and  $\|\mathbf{A}\|$  is the spectral norm of a matrix.

## 3. THE FETI-H METHOD FOR THE HELMHOLTZ EQUATION

In this section, we review the FETI-H method as a starting point in a form suitable for our purposes. For more details, see [3, 4, 5].

Consider a time harmonic acoustic scattering problem in a bounded domain  $\Omega \subset \mathbb{R}^n$ ,  $n = 2$  or  $3$ , filled with fluid with speed of sound  $c_f$  and vibrating at

**FIG. 1.** Model 2D Problem

angular frequency  $\omega$ . The scatterer occupies the domain  $\Omega_e \subset \overline{\Omega_e} \subset \Omega$ , and, in this section, the scatterer is rigid. The fluid domain is  $\Omega_f = \Omega \setminus \overline{\Omega_e}$ , cf., Fig. 1. Let  $\partial\Omega$  be decomposed into disjoint subsets  $\partial\Omega = \Gamma_d \cup \Gamma_n \cup \Gamma_a$ .

The fluid pressure amplitude  $p$  is governed by the Helmholtz equation,

$$\Delta p + k^2 p = 0 \text{ in } \Omega_f, \quad (1)$$

where  $k = \omega/c_f$ , with the boundary conditions

$$p = p_0 \text{ on } \Gamma_d, \quad \frac{\partial p}{\partial \nu} = 0 \text{ on } \Gamma_n, \quad \frac{\partial p}{\partial \nu} + ikp = 0 \text{ on } \Gamma_a, \quad (2)$$

and

$$\frac{\partial p}{\partial \nu} = n \text{ on } \partial\Omega_e. \quad (3)$$

The domain  $\Omega_f$  is decomposed into nonoverlapping subdomains

$$\overline{\Omega_f} = \bigcup_{s=1}^{N_f} \overline{\Omega_f^s}. \quad (4)$$

The normal to  $\partial\Omega_f^s$  is denoted by  $\nu^s$ . It is well-known that under reasonable conditions, the equation (1) is equivalent to the decomposed form  $\Delta p^s + k^2 p^s = 0$

in  $\Omega_f^s$ ,  $s = 1, \dots, N_f$ , with the continuity conditions for  $p$  and its normal derivative on the interfaces between the subdomains,

$$p^s = p^t, \quad \frac{\partial p^s}{\partial \nu^s} = -\frac{\partial p^t}{\partial \nu^t}, \quad \text{on } \partial\Omega_s \cap \partial\Omega_t. \quad (5)$$

Multiplying (1) by a test function  $q$  and integrating by parts using the boundary conditions, one obtains the standard variational form,

$$p - p_0 \in V_f, \quad -\int_{\Omega_f} \nabla p \cdot \nabla q + k^2 \int_{\Omega_f} p q - ik \int_{\Gamma_a} p q = \int_{\partial\Omega_e} n p, \quad \forall q \in V_f, \quad (6)$$

where  $p_0$  is an extension of the boundary data to a function  $p_0 \in H^1(\Omega_f)$ , and  $V_f = \{q \in H^1(\Omega_f) \mid q = 0 \text{ on } \Gamma_d\}$ . A conforming discretization of (6) is obtained by replacing  $V_f$  by a finite element space  $V_f^h \subset V_f$ . Functions in the finite element space have the representation  $p = \sum_{i=1}^m \mathbf{p}_i \phi_i$ , where  $\{\phi_1, \dots, \phi_m\}$  is a basis of  $V_f^h$ . The discretized system is

$$(-\mathbf{K}_f + k^2 \mathbf{M}_f - ik \mathbf{G}_f) \mathbf{p} = \mathbf{r}, \quad (7)$$

where  $\mathbf{K}_f$ ,  $\mathbf{M}_f$ ,  $\mathbf{G}_f$ ,  $\mathbf{r}$  are the stiffness matrix, the mass matrix, the boundary stiffness matrix, and the right-hand side vector, respectively, given by

$$\begin{aligned} \mathbf{p}^T \mathbf{K}_f \mathbf{q} &= \int_{\Omega_f} \nabla p \cdot \nabla q, & \mathbf{p}^T \mathbf{M}_f \mathbf{q} &= \int_{\Omega_f} p q, & \mathbf{p}^T \mathbf{G}_f \mathbf{q} &= \int_{\Gamma_a} p q, \\ \mathbf{q}^T \mathbf{r} &= -\int_{\Omega_f} \nabla p_0 \cdot \nabla q + k^2 \int_{\Omega_f} p_0 q - ik \int_{\Gamma_a} p_0 q + \int_{\partial\Omega_a} n q. \end{aligned} \quad (8)$$

Let the subdomains  $\Omega_f^s$  consist of union of elements. Define subdomain matrices by subassembly,

$$\mathbf{p}^{sT} \mathbf{K}_f^s \mathbf{q} = \int_{\Omega_f^s} \nabla p \cdot \nabla q, \quad \mathbf{p}^{sT} \mathbf{M}_f^s \mathbf{q}^s = \int_{\Omega_f^s} p q, \quad \mathbf{p}^{sT} \mathbf{G}_f^s \mathbf{q}^s = \int_{\Gamma_a} p q, \quad (9)$$

where  $\mathbf{p}^s$  denotes the vector of the entries of  $p$  that are associated with  $\Omega_f^s$ . We will use block vectors and corresponding partitioned matrices,

$$\hat{\mathbf{p}} = \begin{bmatrix} \mathbf{p}^1 \\ \vdots \\ \mathbf{p}^{N_f} \end{bmatrix}, \quad \hat{\mathbf{K}}_f = \begin{bmatrix} \mathbf{K}_f^1 & \dots & 0 \\ \vdots & \ddots & \vdots \\ 0 & \dots & \mathbf{K}_f^{N_f} \end{bmatrix}, \quad \hat{\mathbf{M}}_f = \begin{bmatrix} \mathbf{M}_f^1 & \dots & 0 \\ \vdots & \ddots & \vdots \\ 0 & \dots & \mathbf{M}_f^{N_f} \end{bmatrix}. \quad (10)$$

Let

$$\mathbf{N}_f = \begin{bmatrix} \mathbf{N}_f^1 \\ \vdots \\ \mathbf{N}_f^{N_f} \end{bmatrix}$$

be the  $0-1$  matrix of the global to local map of the subdomain degrees of freedom, so that  $\hat{\mathbf{p}} = \mathbf{N}_f \mathbf{p}$ . Then the global matrices can be written as assembly of the subdomain matrices,

$$\mathbf{K}_f = \mathbf{N}_f^T \hat{\mathbf{K}}_f \mathbf{N}_f, \quad \mathbf{M}_f = \mathbf{N}_f^T \hat{\mathbf{M}}_f \mathbf{N}_f, \quad \mathbf{G}_f = \mathbf{N}_f^T \hat{\mathbf{G}}_f \mathbf{N}_f. \quad (11)$$

It is easy to find  $\hat{\mathbf{r}}$  so that  $\mathbf{r} = \mathbf{N}_f^T \hat{\mathbf{r}}$ . Then the discrete problem (7) is equivalent to  $(-\hat{\mathbf{K}}_f + k^2 \hat{\mathbf{M}}_f - ik \hat{\mathbf{G}}_f) \hat{\mathbf{p}} = \hat{\mathbf{r}}$ , where  $\mathbf{p} = \mathbf{N}_f^T \hat{\mathbf{p}}$ .

Now choose a matrix  $\mathbf{B}_f = [\mathbf{B}_f^1, \dots, \mathbf{B}_f^{N_f}]$  such that the condition  $\mathbf{B}_f \hat{\mathbf{p}} = 0$  is a discrete version of the first constraint in (5), that is, the condition that the values of the same degrees of freedom on two different subdomains coincide. We assume that  $\mathbf{B}_f \hat{\mathbf{p}} = 0$  if and only if  $\hat{\mathbf{p}} = \mathbf{N}_f \mathbf{p}$  for some  $\mathbf{p}$ . Introducing Lagrange multipliers  $\lambda_f$  for the constraint  $\mathbf{B}_f \hat{\mathbf{p}} = 0$ , we obtain the decomposed problem

$$\begin{bmatrix} -\hat{\mathbf{K}}_f + k^2 \hat{\mathbf{M}}_f - ik \hat{\mathbf{G}}_f & \mathbf{B}_f^T \\ \mathbf{B}_f & 0 \end{bmatrix} \begin{bmatrix} \hat{\mathbf{p}} \\ \lambda_f \end{bmatrix} = \begin{bmatrix} \hat{\mathbf{r}} \\ 0 \end{bmatrix}. \quad (12)$$

It is easy to see that (12) is equivalent to (7) in the sense that  $\mathbf{p}$  is a solution of (7) if and only if  $\hat{\mathbf{p}} = \mathbf{N}_f \mathbf{p}$  solves (12) with some  $\lambda_f$ , cf., [27].

To obtain an iterative substructuring method, we will eliminate the primary variables  $\hat{\mathbf{p}}$  from the system (12) and solve the resulting reduced system iteratively. However, the matrix  $-\hat{\mathbf{K}}_f + k^2 \hat{\mathbf{M}}_f$  may be close to singular due to near-resonance, except for diagonal blocks that correspond to subdomains with the radiation boundary condition. This motivates replacing the intersubdomain continuity conditions (5) by the complex linear combination

$$p_s = p_t, \quad \sigma_{st} ik p_s + \frac{\partial p_s}{\partial \nu_s} = \sigma_{st} ik p_t - \frac{\partial p_t}{\partial \nu_t}, \quad \text{on } \partial \Omega_s \cap \partial \Omega_t, \quad (13)$$

where  $\sigma_f^{st} \in \{0, \pm 1\}$ ,  $\sigma_f^{st} = -\sigma_f^{ts}$ . This means that the decomposed problem (12) is replaced by the *regularized system*

$$\begin{bmatrix} \hat{\mathbf{A}}_f & \mathbf{B}_f^T \\ \mathbf{B}_f & 0 \end{bmatrix} \begin{bmatrix} \hat{\mathbf{p}} \\ \lambda_f \end{bmatrix} = \begin{bmatrix} \hat{\mathbf{r}} \\ 0 \end{bmatrix}, \quad (14)$$

where

$$\hat{\mathbf{A}}_f = -\hat{\mathbf{K}}_f + k^2 \hat{\mathbf{M}}_f - ik \hat{\mathbf{G}}_f + ik \hat{\mathbf{R}}_f, \quad (15)$$

and the regularization matrix  $\hat{\mathbf{R}}_f$  is given by

$$\hat{\mathbf{R}}_f = \begin{bmatrix} \mathbf{R}_f^1 & \dots & 0 \\ \vdots & \ddots & \vdots \\ 0 & \dots & \mathbf{R}_f^{N_f} \end{bmatrix}, \quad \mathbf{p}^{sT} \mathbf{R}_f^s \mathbf{q}^s = \sum_{\substack{t=1 \\ t \neq s}}^{N_f} \sigma_f^{st} \int_{\partial \Omega_f^s \cap \partial \Omega_f^t} pq. \quad (16)$$

Clearly,  $\mathbf{N}_f^T \mathbf{R}_f \mathbf{N}_f = 0$ , that is, the contributions to the subdomain matrices in the subdomain assembly cancel, so (14) and (12) are equivalent. It is shown in [18] that if for a given  $s$ , all  $\sigma_f^{st} \geq 0$  or all  $\sigma_f^{st} \leq 0$  with some  $\sigma_f^{st} \neq 0$ , then  $\hat{\mathbf{A}}_f^s$  is invertible. For details on strategies for choosing  $\sigma_f^{st}$  to guarantee this, see [18].

After eliminating the primary variables by  $\hat{\mathbf{p}} = \hat{\mathbf{A}}_f^{-1}(\hat{\mathbf{r}} - \mathbf{B}_f^T \lambda_f)$ , we obtain the *reduced system* for the Lagrange multipliers  $\lambda_f$ ,

$$\mathbf{F}_f \lambda_f = \mathbf{g}_f, \quad \text{where} \quad \mathbf{F}_f = -\mathbf{B}_f \hat{\mathbf{A}}_f^{-1} \mathbf{B}_f^T, \quad \mathbf{g}_f = \mathbf{B}_f \hat{\mathbf{A}}_f^{-1} \hat{\mathbf{r}}. \quad (17)$$

The reduced system (17) is solved iteratively, with preconditioning by subspace correction, using a coarse space with few degrees of freedom per subdomain as follows.

Because the same iterative method applies to generalizations to elasticity and to the coupled problem, we drop the subscript  $f$  and denote the vector of unknowns by  $\mathbf{x}$  rather than  $\mathbf{p}$  and  $\mathbf{b}$  rather than  $\mathbf{g}$ .

Let  $\mathbf{Q}$  be a matrix with the same number of rows as  $\mathbf{F}$ . The columns of  $\mathbf{Q}$  span the *coarse space*. FETI-H enforces the condition that the residual is orthogonal to the coarse space,

$$\mathbf{Q}^T(\mathbf{F}\mathbf{x} - \mathbf{b}) = 0, \quad (18)$$

by adding a correction from the coarse space in each iteration, which results in the preconditioned system

$$\mathbf{P}\mathbf{F}\mathbf{x} = \mathbf{P}\mathbf{b}, \quad (19)$$

where

$$\mathbf{P} = \mathbf{I} - \mathbf{Q}(\mathbf{Q}^T \mathbf{F} \mathbf{Q})^{-1} \mathbf{Q}^T \mathbf{F}. \quad (20)$$

Since it follows from (19) that  $\mathbf{F}\mathbf{x} - \mathbf{b} \in \text{Range } \mathbf{Q}$ , the equations (18) and (19) together imply that  $\mathbf{F}\mathbf{x} = \mathbf{b}$ .

The system (19) is solved by Krylov space iterations. The initial approximation is chosen to satisfy (18). Since all increments are in the span of residuals of (19) and  $\mathbf{Q}^T \mathbf{F} \mathbf{P} = 0$ , all iterates satisfy (18).

For the Helmholtz equation in  $\Omega_f$ , the matrix  $\mathbf{Q} = \mathbf{Q}_f$  is chosen as

$$\mathbf{Q}_f = \mathbf{B}_f \mathbf{Y}_f, \quad \mathbf{Y}_f = \begin{bmatrix} \mathbf{Y}_f^1 & \dots & 0 \\ \vdots & \ddots & \vdots \\ 0 & \dots & \mathbf{Y}_f^{N_f} \end{bmatrix}, \quad (21)$$

where the columns of  $\mathbf{Y}_f^s$  are finite element interpolants in  $\Omega^s$  of plane waves  $y_k(x) = e^{ikx \cdot d_k}$  in several directions  $|d_k| = 1$ . In 2D, we choose an even number of directions equidistant on the unit circumference. Since with each direction, the opposite direction is also included, the column space of  $\mathbf{Q}$  is same as the column space of the complex conjugate of  $\mathbf{Q}$ , so it does not matter if the transpose or the conjugate transpose are used in (18).

#### 4. EXTENSION TO ELASTIC SCATTERING

Consider the time harmonic elastodynamic equation

$$\nabla \cdot \boldsymbol{\tau} + \omega^2 \rho_e u = 0 \quad \text{in} \quad \Omega_e, \quad (22)$$

with natural boundary conditions

$$\boldsymbol{\tau} \cdot \boldsymbol{\nu} = -p\boldsymbol{\nu} \text{ on } \partial\Omega_e, \quad (23)$$

Here,  $u$  is the displacement,  $\boldsymbol{\tau}$  is the stress tensor,  $\rho_e$  is the density of the solid, and  $p$  is given boundary data. For simplicity, we consider an isotropic homogeneous material with

$$\boldsymbol{\tau} = \lambda I(\nabla \cdot \boldsymbol{u}) + 2\mu \boldsymbol{e}(u), \quad \boldsymbol{e}_{ij}(u) = \frac{1}{2} \left( \frac{\partial u_i}{\partial x_j} + \frac{\partial u_j}{\partial x_i} \right), \quad (24)$$

where  $\lambda$  and  $\mu$  are the Lamé coefficients of the solid. Similarly as in the previous section,  $\Omega_e$  is decomposed into non-overlapping subdomains  $\Omega_e^1, \dots, \Omega_e^{N_e}$ , and, under reasonable conditions [28], equation (22) is equivalent to the decomposed form  $\nabla \cdot \boldsymbol{\tau}^s + \omega^2 \rho_e u^s = 0$  in  $\Omega_e^s$ ,  $s = 1, \dots, N_e$ , with the continuity of the displacement and the traction on intersubdomain interfaces,

$$u_s = u_t, \quad \boldsymbol{\tau}_s \cdot \boldsymbol{\nu}_s = -\boldsymbol{\tau}_t \cdot \boldsymbol{\nu}_t, \quad \text{on } \partial\Omega_e^s \cap \partial\Omega_e^t. \quad (25)$$

We have the standard variational formulation of (22) for  $u \in V_e = (H^1(\Omega_e))^n$ ,

$$-\int_{\Omega_e} (\lambda(\nabla \cdot \boldsymbol{u})(\nabla \cdot \boldsymbol{v}) + 2\mu \boldsymbol{e}(u) : \boldsymbol{e}(v)) + \omega^2 \int_{\Omega_e} \rho_e \boldsymbol{u} \cdot \boldsymbol{v} - \int_{\Gamma} p(\boldsymbol{\nu} \cdot \boldsymbol{v}) = 0, \quad \forall \boldsymbol{v} \in V_e,$$

the discretization

$$(-\mathbf{K}_e + \omega^2 \mathbf{M}_e) \mathbf{u} = \mathbf{s},$$

with the matrices and the right-hand side defined by

$$\mathbf{u}^T \mathbf{K}_e \mathbf{v} = \int_{\Omega_e} (\lambda(\nabla \cdot \boldsymbol{u})(\nabla \cdot \boldsymbol{v}) + 2\mu \boldsymbol{e}(u) : \boldsymbol{e}(v)), \quad (26)$$

$$\mathbf{u}^T \mathbf{M}_e \mathbf{v} = \int_{\Omega_e} \rho_e (\boldsymbol{u} \cdot \boldsymbol{v}), \quad \mathbf{u}^T \mathbf{s} = \int_{\Gamma} q(\boldsymbol{\nu} \cdot \boldsymbol{v}), \quad (27)$$

the block form of the solution and the subdomain matrices

$$\hat{\mathbf{u}} = \begin{bmatrix} \mathbf{u}^1 \\ \vdots \\ \mathbf{u}^{N_e} \end{bmatrix}, \quad \hat{\mathbf{K}}_e = \begin{bmatrix} \mathbf{K}_e^1 & \dots & 0 \\ \vdots & \ddots & \vdots \\ 0 & \dots & \mathbf{K}_e^{N_e} \end{bmatrix}, \quad \hat{\mathbf{M}}_e = \begin{bmatrix} \mathbf{M}_e^1 & \dots & 0 \\ \vdots & \ddots & \vdots \\ 0 & \dots & \mathbf{M}_e^{N_e} \end{bmatrix}, \quad (28)$$

the matrix of the global to local mapping  $\mathbf{N}_e$ , the assembly of subdomain matrices,

$$\mathbf{K}_e = \mathbf{N}_e^T \hat{\mathbf{K}}_e \mathbf{N}_e, \quad \mathbf{M}_e = \mathbf{N}_e^T \hat{\mathbf{M}}_e \mathbf{N}_e, \quad (29)$$

the constraint matrix  $\mathbf{B}_e$  such that  $\mathbf{B}_e \hat{\mathbf{u}} = 0$  if and only if  $\hat{\mathbf{u}} = \mathbf{N}_e \mathbf{u}$  for some  $u$ , and the decomposed problem

$$\begin{bmatrix} -\hat{\mathbf{K}}_e + k^2 \hat{\mathbf{M}}_e & \mathbf{B}_e^T \\ \mathbf{B}_e & 0 \end{bmatrix} \begin{bmatrix} \hat{\mathbf{u}} \\ \boldsymbol{\lambda}_e \end{bmatrix} = \begin{bmatrix} \hat{\mathbf{s}} \\ 0 \end{bmatrix}, \quad (30)$$

where  $\mathbf{s} = \mathbf{N}_e^T \hat{\mathbf{s}}$ .

To avoid nearly singular matrices in the subdomains, the intersubdomain conditions are replaced by their complex linear combination [17]

$$u_s = u_t, \quad \sigma_{st} i \omega \rho_e u_s + \tau_s \cdot \nu_s = \sigma_{st} i \omega \rho_e u_t - \tau_t \cdot \nu_t, \quad \text{on } \partial\Omega_e^s \cap \partial\Omega_e^t,$$

where  $\sigma_e^{st} \in \{0, \pm 1\}$ ,  $\sigma_e^{st} = -\sigma_e^{ts}$ , and we obtain the regularized system

$$\begin{bmatrix} \hat{\mathbf{A}}_e & \mathbf{B}_e^T \\ \mathbf{B}_e & 0 \end{bmatrix} \begin{bmatrix} \hat{\mathbf{u}} \\ \lambda_e \end{bmatrix} = \begin{bmatrix} \hat{\mathbf{r}} \\ 0 \end{bmatrix}, \quad (31)$$

where

$$\hat{\mathbf{A}}_e = -\hat{\mathbf{K}}_e + \omega^2 \hat{\mathbf{M}}_e + i\omega \hat{\mathbf{R}}_e, \quad (32)$$

and

$$\hat{\mathbf{R}}_e = \begin{bmatrix} \mathbf{R}_e^1 & \dots & 0 \\ \vdots & \ddots & \vdots \\ 0 & \dots & \mathbf{R}_e^{N_e} \end{bmatrix}, \quad \mathbf{u}^s T \mathbf{R}_e^s \mathbf{v}^s = \rho_e \sum_{\substack{t=1 \\ t \neq s}}^{N_e} \sigma_e^{st} \int_{\partial\Omega_e^s \cap \partial\Omega_e^t} (n \cdot u)(n \cdot v).$$

After elimination of  $\hat{\mathbf{u}}$ , the reduced system with the matrix

$$\mathbf{F}_e \lambda_e = \mathbf{g}_e, \quad \text{where } \mathbf{F}_e = -\mathbf{B}_e \hat{\mathbf{A}}_e^{-1} \mathbf{B}_e^T, \quad (33)$$

can be solved iteratively in the same way as in the previous section, with the matrix of the coarse space generators

$$\mathbf{Q}_e = \mathbf{B}_e \mathbf{Y}_e, \quad \mathbf{Y}_e = \begin{bmatrix} \mathbf{Y}_e^1 & \dots & 0 \\ \vdots & \ddots & \vdots \\ 0 & \dots & \mathbf{Y}_e^{N_e} \end{bmatrix}, \quad (34)$$

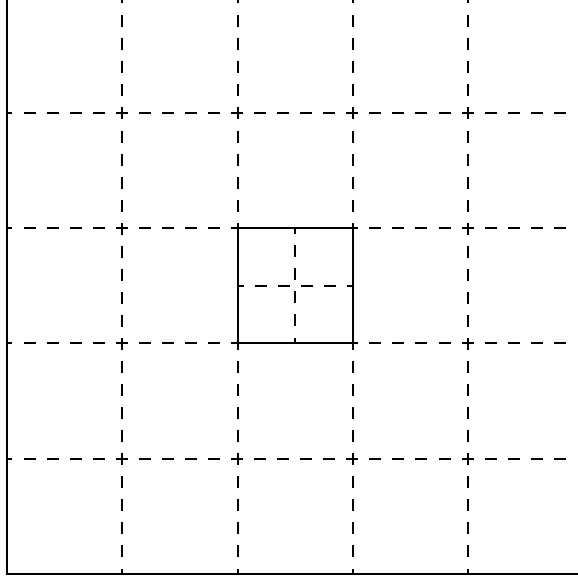
with the columns of  $\mathbf{Y}_e^s$  being interpolants of pressure and shear plane waves in  $\Omega_e^s$ , cf., e.g., [29].

## 5. ITERATIVE SUBSTRUCTURING FOR COUPLED PROBLEM

We are now ready to consider the coupled problem. The fluid pressure in  $\Omega_f$  satisfies the Helmholtz equation (1) and the boundary conditions (2). The displacement of the solid in  $\Omega_e$  satisfies the elastodynamic equation (22). Let  $\Gamma = \partial\Omega_e$  be the wet interface. On  $\Gamma$ , the fluid pressure and the solid displacement satisfy the interface conditions

$$\nu \cdot u = \frac{1}{\rho_f \omega^2} \frac{\partial p}{\partial \nu}, \quad \tau \cdot \nu = -p\nu, \quad (35)$$

where  $\rho_f$  is the fluid density. The equations in (35) model the continuity of normal displacement and the balance of forces, respectively, cf., e.g., [29].

**FIG. 2.** Model 2D Problem Decomposed in 5x5 Fluid and 2x2 Solid Subdomains

Multiplying the equations (1) and (22) by test functions and integrating by parts using the boundary and the interface conditions, we obtain the standard variational form [30]

$$\begin{aligned}
 & p - p_0 \in V_f, \quad u \in V_e, \\
 & - \int_{\Omega_f} \nabla p \cdot \nabla q + k^2 \int_{\Omega_f} pq - ik \int_{\Gamma_a} pq - \omega^2 \int_{\Gamma} \rho_f (\nu \cdot u) q = 0, \\
 & - \int_{\Omega_e} (\lambda (\nabla \cdot u) (\nabla \cdot v) + 2\mu e(u) : e(v)) + \omega^2 \int_{\Omega_e} \rho_e u \cdot v - \int_{\Gamma} p (\nu \cdot v) = 0, \\
 & \forall q \in V_f, \quad v \in V_e.
 \end{aligned}$$

The finite element discretization is

$$\begin{bmatrix} -\mathbf{K}_f + k^2 \mathbf{M}_f - ik \mathbf{G}_f & -\rho_f \omega^2 \mathbf{T} \\ -\rho_f \omega^2 \mathbf{T}^T & \rho_f \omega^2 (-\mathbf{K}_e + \omega^2 \mathbf{M}_e) \end{bmatrix} \begin{bmatrix} \mathbf{p} \\ \mathbf{u} \end{bmatrix} = \begin{bmatrix} \mathbf{r} \\ 0 \end{bmatrix}, \quad (36)$$

where  $\mathbf{K}_f$  and  $\mathbf{M}_f$  are as in (8),  $\mathbf{K}_e$  and  $\mathbf{M}_e$  are as in (26), (27), and  $\mathbf{T}$  is given by

$$\mathbf{q}^T \mathbf{T} \mathbf{v} = \int_{\Gamma} q (\nu \cdot v).$$

The second equation in (36) was multiplied  $\rho_f \omega^2$  to symmetrize the system.

The fluid and the solid domains are decomposed into nonoverlapping subdomains, cf., Fig. 2. Again, we assume that the subdomains that are unions of elements. Introducing Lagrange multipliers  $\lambda_f$  and  $\lambda_e$  for the constraints  $\mathbf{B}_f \mathbf{p} = 0$  and

$\mathbf{B}_e \mathbf{u} = 0$ , we get the system of linear equations in block form,

$$\begin{bmatrix} -\hat{\mathbf{K}}_f + k^2 \hat{\mathbf{M}}_f - ik \hat{\mathbf{G}} & -\omega^2 \rho_f \hat{\mathbf{T}} & \mathbf{B}_f^T & 0 \\ -\omega^2 \rho_f \hat{\mathbf{T}}^T & \omega^2 \rho_f (-\hat{\mathbf{K}}_e + \omega^2 \hat{\mathbf{M}}_e) & 0 & \mathbf{B}_e^T \\ \mathbf{B}_f & 0 & 0 & 0 \\ 0 & \mathbf{B}_e & 0 & 0 \end{bmatrix} \begin{bmatrix} \hat{\mathbf{p}} \\ \hat{\mathbf{u}} \\ \lambda_f \\ \lambda_e \end{bmatrix} = \begin{bmatrix} \hat{\mathbf{r}} \\ 0 \\ 0 \\ 0 \end{bmatrix}, \quad (37)$$

where  $\hat{\mathbf{K}}_f$ ,  $\hat{\mathbf{M}}_f$ ,  $\hat{\mathbf{G}}_f$ ,  $\hat{\mathbf{K}}_e$ , and  $\hat{\mathbf{M}}_e$  are given by (10), (28), and

$$\hat{\mathbf{T}} = \begin{bmatrix} \mathbf{T}^{11} & \dots & \mathbf{T}^{1,N_e} \\ \vdots & \ddots & \vdots \\ \mathbf{T}^{N_f,1} & \dots & \mathbf{T}^{N_f,N_e} \end{bmatrix}, \quad \mathbf{q}^{st} \hat{\mathbf{T}}^{st} \mathbf{v}^t = \int_{\Gamma \cap \partial \Omega_f^s \cap \partial \Omega_e^t} q(\nu \cdot \mathbf{v}).$$

Again, the system (37) is equivalent to (36). Adding the regularization matrices on the interfaces between the solid subdomains, we obtain the equivalent regularized system

$$\begin{bmatrix} \hat{\mathbf{A}}_f & -\omega^2 \rho_f \hat{\mathbf{T}} & \mathbf{B}_f^T & 0 \\ -\omega^2 \rho_f \hat{\mathbf{T}}^T & \omega^2 \rho_f \hat{\mathbf{A}}_e & 0 & \mathbf{B}_e^T \\ \mathbf{B}_f & 0 & 0 & 0 \\ 0 & \mathbf{B}_e & 0 & 0 \end{bmatrix} \begin{bmatrix} \hat{\mathbf{p}} \\ \hat{\mathbf{u}} \\ \lambda_f \\ \lambda_e \end{bmatrix} = \begin{bmatrix} \hat{\mathbf{r}} \\ 0 \\ 0 \\ 0 \end{bmatrix}, \quad (38)$$

where  $\hat{\mathbf{A}}_f$  and  $\hat{\mathbf{A}}_e$  are given by (15) and (32), respectively.

At this point, we would like to eliminate the primary variables  $\hat{\mathbf{p}}$  and  $\hat{\mathbf{u}}$  to obtain a system in the Lagrange multipliers  $\lambda_f$ ,  $\lambda_e$  only. For the coupled system, however, the elimination does not reduce to independent problems in all subdomains because subdomains across the wet interface are coupled via the matrix  $\hat{\mathbf{T}}$ . So, first we augment the system by duplicating the degrees of freedom on the wet interface as follows.

Since the value of  $\hat{\mathbf{T}} \hat{\mathbf{u}}$  depends only on the entries of  $\hat{\mathbf{u}}$  that correspond to degrees of freedom on  $\Gamma$ , we have  $\hat{\mathbf{T}} \hat{\mathbf{u}} = \hat{\mathbf{T}} \mathbf{J}_e \hat{\mathbf{u}}_\Gamma$ , where  $\hat{\mathbf{u}}_\Gamma = \mathbf{J}_e^T \hat{\mathbf{u}}$  and  $\mathbf{J}_e$  is the matrix of the operator of embedding a subvector  $\hat{\mathbf{u}}_\Gamma$  into  $\hat{\mathbf{u}}$  by adding zero entries. Similarly,  $\hat{\mathbf{T}}^T \hat{\mathbf{p}} = \hat{\mathbf{T}}^T \mathbf{J}_f \hat{\mathbf{p}}_\Gamma$ , where  $\hat{\mathbf{p}}_\Gamma = \mathbf{J}_f^T \hat{\mathbf{p}}$ . Adding  $\mathbf{p}_\Gamma$  and  $\mathbf{u}_\Gamma$  as new variables, we obtain the *augmented system* equivalent to (38),

$$\begin{bmatrix} \hat{\mathbf{A}}_f & 0 & \mathbf{B}_f^T & 0 & 0 & -\omega^2 \rho_f \hat{\mathbf{T}} \mathbf{J}_e \\ 0 & \omega^2 \rho_f \hat{\mathbf{A}}_e & 0 & \mathbf{B}_e^T & -\omega^2 \rho_f \hat{\mathbf{T}}^T \mathbf{J}_f & 0 \\ \mathbf{B}_f & 0 & 0 & 0 & 0 & 0 \\ 0 & \mathbf{B}_e & 0 & 0 & 0 & 0 \\ \mathbf{J}_f^T & 0 & 0 & 0 & -\mathbf{I} & 0 \\ 0 & \mathbf{J}_e^T & 0 & 0 & 0 & -\mathbf{I} \end{bmatrix} \begin{bmatrix} \hat{\mathbf{p}} \\ \hat{\mathbf{u}} \\ \lambda_f \\ \lambda_e \\ \hat{\mathbf{p}}_\Gamma \\ \hat{\mathbf{u}}_\Gamma \end{bmatrix} = \begin{bmatrix} \hat{\mathbf{r}} \\ 0 \\ 0 \\ 0 \\ 0 \\ 0 \end{bmatrix}. \quad (39)$$

Because the variables in a coupled system typically have vastly different scales, we use symmetric diagonal scaling to get the scaled system

$$\begin{bmatrix} \tilde{\mathbf{A}}_f & 0 & \tilde{\mathbf{B}}_f^T & 0 & 0 & -\tilde{\mathbf{T}}\mathbf{J}_e \\ 0 & \tilde{\mathbf{A}}_e & 0 & \tilde{\mathbf{B}}_e^T & -\tilde{\mathbf{T}}^T\mathbf{J}_f & 0 \\ \tilde{\mathbf{B}}_f & 0 & 0 & 0 & 0 & 0 \\ 0 & \tilde{\mathbf{B}}_e & 0 & 0 & 0 & 0 \\ \mathbf{J}_f^T & 0 & 0 & 0 & -\mathbf{I} & 0 \\ 0 & \mathbf{J}_e^T & 0 & 0 & 0 & -\mathbf{I} \end{bmatrix} \begin{bmatrix} \tilde{\mathbf{p}} \\ \tilde{\mathbf{u}} \\ \tilde{\lambda}_f \\ \tilde{\lambda}_e \\ \tilde{\mathbf{p}}_\Gamma \\ \tilde{\mathbf{u}}_\Gamma \end{bmatrix} = \begin{bmatrix} \tilde{\mathbf{r}} \\ 0 \\ 0 \\ 0 \\ 0 \\ 0 \end{bmatrix}, \quad (40)$$

where the matrices and the vectors scale as

$$\tilde{\mathbf{A}}_f = \mathbf{D}_f \hat{\mathbf{A}}_f \mathbf{D}_f, \quad \tilde{\mathbf{A}}_e = \omega^2 \rho_f \mathbf{D}_e \hat{\mathbf{A}}_e \mathbf{D}_e, \quad \tilde{\mathbf{T}} = \omega^2 \rho_f \mathbf{D}_f \hat{\mathbf{T}} \mathbf{D}_e, \quad (41)$$

$$\tilde{\mathbf{B}}_f = \mathbf{E}_f \mathbf{B}_f \mathbf{D}_f, \quad \tilde{\mathbf{B}}_e = \mathbf{E}_e \mathbf{B}_e \mathbf{D}_e, \quad \tilde{\mathbf{r}} = \mathbf{D}_f \hat{\mathbf{r}}, \quad (42)$$

$$\tilde{\mathbf{p}} = \mathbf{D}_f \hat{\mathbf{p}}, \quad \tilde{\mathbf{u}} = \mathbf{D}_e \hat{\mathbf{u}}, \quad \tilde{\lambda}_f = \mathbf{D}_f \hat{\lambda}_f, \quad \tilde{\lambda}_e = \mathbf{D}_e \hat{\lambda}_e. \quad (43)$$

The scaling matrices  $\mathbf{D}_f$ ,  $\mathbf{D}_e$ ,  $\mathbf{E}_f$ , and  $\mathbf{E}_e$  are diagonal with positive diagonal entries. We first choose  $\mathbf{D}_f$  and  $\mathbf{D}_e$  so that the absolute values of the diagonal entries of  $\tilde{\mathbf{A}}_f$  and  $\tilde{\mathbf{A}}_e$  are one. Then the matrices  $\mathbf{E}_f$  and  $\mathbf{E}_e$  are defined by the property that the  $\ell^2$  norms of the columns of  $\tilde{\mathbf{B}}_e$  and  $\tilde{\mathbf{B}}_f$  are one. It is easy to see that the scaling results in a dimensionless system. In addition, the scaling reveals numerical near decoupling of the fluid and the elastic problem, cf., Section 6 below.

We now eliminate the variables  $\tilde{\mathbf{p}}$  and  $\tilde{\mathbf{u}}$  from the augmented system (40) and solve the resulting reduced system iteratively. Computing  $\tilde{\mathbf{p}}$  and  $\tilde{\mathbf{u}}$  from the first two equations in (40) gives

$$\tilde{\mathbf{p}} = \tilde{\mathbf{A}}_f^{-1}(\tilde{\mathbf{r}} - \tilde{\mathbf{B}}_f^T \tilde{\lambda}_f + \tilde{\mathbf{T}}\mathbf{J}_e \tilde{\mathbf{u}}_\Gamma), \quad (44)$$

$$\tilde{\mathbf{u}} = \tilde{\mathbf{A}}_e^{-1}(-\tilde{\mathbf{B}}_e^T \tilde{\lambda}_e + \tilde{\mathbf{T}}^T \mathbf{J}_f \tilde{\mathbf{p}}_\Gamma). \quad (45)$$

Substituting  $\tilde{\mathbf{p}}$  and  $\tilde{\mathbf{u}}$  from (44), (45) into the rest of the equations in (40), we obtain the reduced system

$$\mathbf{F}\mathbf{x} = \mathbf{b}, \quad (46)$$

where

$$\mathbf{F} = \begin{bmatrix} -\tilde{\mathbf{B}}_f \tilde{\mathbf{A}}_f^{-1} \tilde{\mathbf{B}}_f^T & 0 & 0 & \tilde{\mathbf{B}}_f \tilde{\mathbf{A}}_f^{-1} \tilde{\mathbf{T}}\mathbf{J}_e \\ 0 & -\tilde{\mathbf{B}}_e \tilde{\mathbf{A}}_e^{-1} \tilde{\mathbf{B}}_e^T & \tilde{\mathbf{B}}_e \tilde{\mathbf{A}}_e^{-1} \tilde{\mathbf{T}}^T \mathbf{J}_f & 0 \\ -\mathbf{J}_f^T \tilde{\mathbf{A}}_f^{-1} \tilde{\mathbf{B}}_f^T & 0 & -\mathbf{I} & \mathbf{J}_f^T \tilde{\mathbf{A}}_f^{-1} \tilde{\mathbf{T}}\mathbf{J}_e \\ 0 & -\mathbf{J}_e \tilde{\mathbf{A}}_e^{-1} \tilde{\mathbf{B}}_e^T & \mathbf{J}_e \tilde{\mathbf{A}}_e^{-1} \tilde{\mathbf{T}}^T \mathbf{J}_f & -\mathbf{I} \end{bmatrix}, \quad (47)$$

and

$$\mathbf{x} = \begin{bmatrix} \lambda_f \\ \lambda_e \\ \tilde{\mathbf{p}}_\Gamma \\ \tilde{\mathbf{u}}_\Gamma \end{bmatrix}, \quad \mathbf{b} = \begin{bmatrix} -\tilde{\mathbf{B}}_f \tilde{\mathbf{A}}_f^{-1} \tilde{\mathbf{r}} \\ 0 \\ \mathbf{J}_f^T \tilde{\mathbf{A}}_f^{-1} \tilde{\mathbf{r}} \\ 0 \end{bmatrix}.$$

Evaluating the matrix vector product  $\mathbf{F}\mathbf{x}$  requires the solution of one independent problem per subdomain, because

$$\mathbf{F} \begin{bmatrix} \lambda_f \\ \lambda_e \\ \tilde{\mathbf{p}}_\Gamma \\ \tilde{\mathbf{u}}_\Gamma \end{bmatrix} = \begin{bmatrix} \tilde{\mathbf{B}}_f \tilde{\mathbf{q}} \\ \tilde{\mathbf{B}}_e \tilde{\mathbf{v}} \\ \mathbf{J}_f^T \tilde{\mathbf{q}} - \tilde{\mathbf{p}}_\Gamma \\ \mathbf{J}_e^T \tilde{\mathbf{v}} - \tilde{\mathbf{u}}_\Gamma \end{bmatrix}, \quad \text{where} \quad \begin{cases} \tilde{\mathbf{q}} = \tilde{\mathbf{A}}_f^{-1}(-\tilde{\mathbf{B}}_f^T \tilde{\lambda}_f + \tilde{\mathbf{T}} \mathbf{J}_e \tilde{\mathbf{u}}_\Gamma), \\ \tilde{\mathbf{v}} = \tilde{\mathbf{A}}_e^{-1}(-\tilde{\mathbf{B}}_e^T \tilde{\lambda}_e + \tilde{\mathbf{T}}^T \mathbf{J}_f \tilde{\mathbf{p}}_\Gamma). \end{cases}$$

The present method consists of solving the linear system (46) by GMRES. For the coupled problem, the matrix  $\mathbf{Q}$  of coarse space generators is

$$\mathbf{Q} = \begin{bmatrix} \mathbf{D}_f \mathbf{B}_f \mathbf{Y}_f & 0 & 0 & 0 \\ 0 & \mathbf{D}_e \mathbf{B}_e \mathbf{Y}_e & 0 & 0 \\ 0 & 0 & \mathbf{D}_f \mathbf{J}_f^T \mathbf{Z}_f & 0 \\ 0 & 0 & 0 & \mathbf{D}_e \mathbf{J}_e^T \mathbf{Z}_e \end{bmatrix}, \quad (48)$$

where  $\mathbf{Y}_f$  and  $\mathbf{Y}_e$  are given by (21) and (34), respectively, as matrices of columns that are discrete representation of plane waves in the subdomains. The matrices  $\mathbf{Z}_f$  and  $\mathbf{Z}_e$  are of the same form as  $\mathbf{Y}_f$  and  $\mathbf{Y}_e$ , respectively. Because the multiplication by  $\mathbf{J}_f^T$  and  $\mathbf{J}_e^T$  selects only values of degrees of freedoms on the wet interface, the only blocks of  $\mathbf{Z}_f$  and  $\mathbf{Z}_e$  that contribute to  $\mathbf{Q}$  are blocks for subdomains adjacent to the wet interface.

## 6. EXPLANATION OF CONVERGENCE PROPERTIES

Convergence of the method can be explained by an analysis of the spectrum of the iteration operator. From well-known properties of Krylov space methods [31], it follows that in  $m$  iterations, the residual is reduced by the factor of at least  $Cr(m)$ , where

$$r(m) = \min_{\substack{\deg(p)=m \\ p(0)=1}} \max_{\substack{\lambda \in \sigma(\mathbf{P}\mathbf{F}) \\ \lambda \neq 0}} |p(\lambda)|.$$

Here, the minimum is taken over complex polynomials and the maximum over the eigenvalues of  $\mathbf{P}\mathbf{F}$ . It is well-known that  $r(m)$  decreases fast with  $m$  if the eigenvalues are clustered around a point other than zero. Such clustering has been observed in FETI-H [3].

We argue that because of the form of the operator  $\mathbf{F}$ , the same clustering can be expected for the coupled problem. Aside from the diagonal scaling, the first diagonal block of  $\mathbf{F}$  in (47) is same as in the FETI-H method for the Helmholtz equation, cf. (17) and second diagonal block is same as in the extension of FETI-H for the elastodynamic problem, cf., (33). FETI-H is known to converge fast, so one can expect that on the subspace defined by the coarse correction, these two diagonal blocks will be well conditioned. The off-diagonal blocks all contain the inverse of  $\tilde{\mathbf{A}}_f$  or  $\tilde{\mathbf{A}}_e$ , which are discretizations of differential operators. Hence, the off-diagonal blocks resemble discretizations of compact operators, and the structure of equation (46) resembles discretization of a Fredholm integral equation of the second kind, which is well conditioned because its eigenvalues cluster about a point different from zero. Such clustering is indeed observed computationally.

For a very rigid scatterer, the problem becomes numerically decoupled in the limit. Indeed, if the Lamé coefficient  $\mu \rightarrow +\infty$ , the scaling matrix  $\mathbf{D}_e \rightarrow 0$ , hence from (41),  $\tilde{\mathbf{T}} \rightarrow 0$ , and one has

$$\mathbf{F} \rightarrow \begin{bmatrix} -\tilde{\mathbf{B}}_f \tilde{\mathbf{A}}_f^{-1} \tilde{\mathbf{B}}_f^T & 0 & 0 & 0 \\ 0 & -\tilde{\mathbf{B}}_e \tilde{\mathbf{A}}_e^{-1} \tilde{\mathbf{B}}_e^T & 0 & 0 \\ -\mathbf{J}_f^T \tilde{\mathbf{A}}_f^{-1} \tilde{\mathbf{B}}_f^T & 0 & -\mathbf{I} & 0 \\ 0 & -\mathbf{J}_e \tilde{\mathbf{A}}_e^{-1} \tilde{\mathbf{B}}_e^T & 0 & -\mathbf{I} \end{bmatrix}, \text{ as } \mu \rightarrow +\infty. \quad (49)$$

We show that the decoupling indicated by (49) takes place for a wide range of parameters important in practice. Assume that the mesh is quasiuniform with characteristic spacing  $h$ . Then  $\|T\| \approx h^{n-1}$ . Further assuming that  $kh \ll 1$ , which should be the case for approximation reasons, it is easy to see that  $\|\mathbf{D}_f\| \approx (h^{n-2})^{-1/2}$ . Similarly, if  $\omega^2 h^2 \rho_e \ll \mu$ , we have  $\|\mathbf{D}_e\| \approx (\omega^2 \rho_f \mu h^{n-2})^{-1/2}$ , and it follows that

$$\begin{aligned} \|\tilde{\mathbf{T}}\| &= \omega^2 \rho_f \|\mathbf{D}_f \hat{\mathbf{T}} \mathbf{D}_e\| \leq \omega^2 \rho_f \|\mathbf{D}_f\| \|\hat{\mathbf{T}}\| \|\mathbf{D}_e\| \\ &\approx \omega^2 \rho_f (h^{n-2})^{-1/2} h^{n-1} (\omega^2 \rho_f \mu h^{n-2})^{-1/2} \\ &= \omega h \rho_f^{1/2} \mu^{-1/2} = khc_f \rho_f^{1/2} \mu^{-1/2}. \end{aligned}$$

Consequently, the system will become numerically decoupled if

$$khc_f \rho_f^{1/2} \mu^{-1/2} \ll 1. \quad (50)$$

In the computations reported in Section 9, the condition (50) is satisfied, because  $khc_f \rho_f^{1/2} \mu^{-1/2}$  was of the order of at most  $10^{-3}$ .

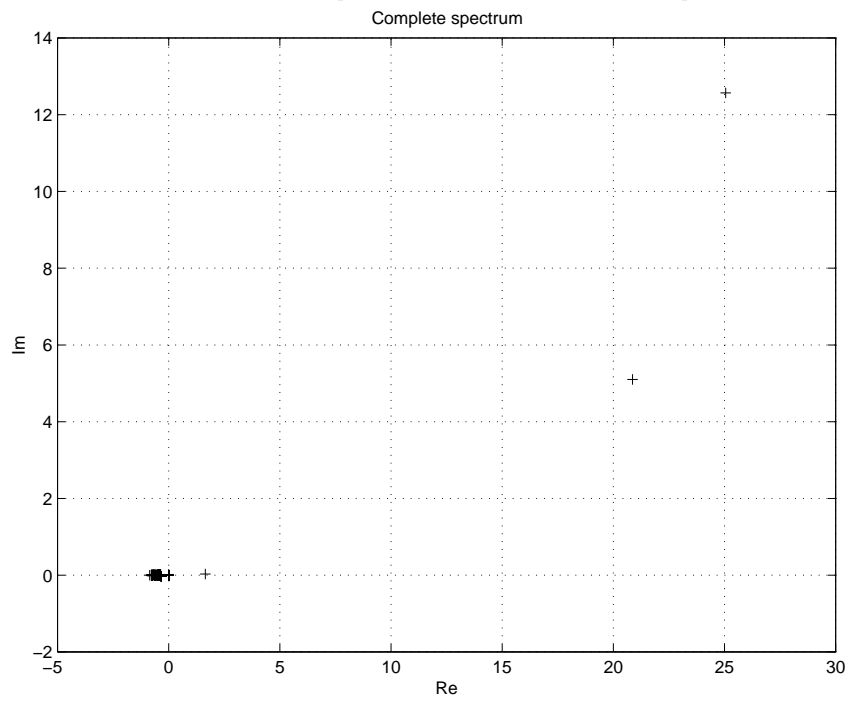
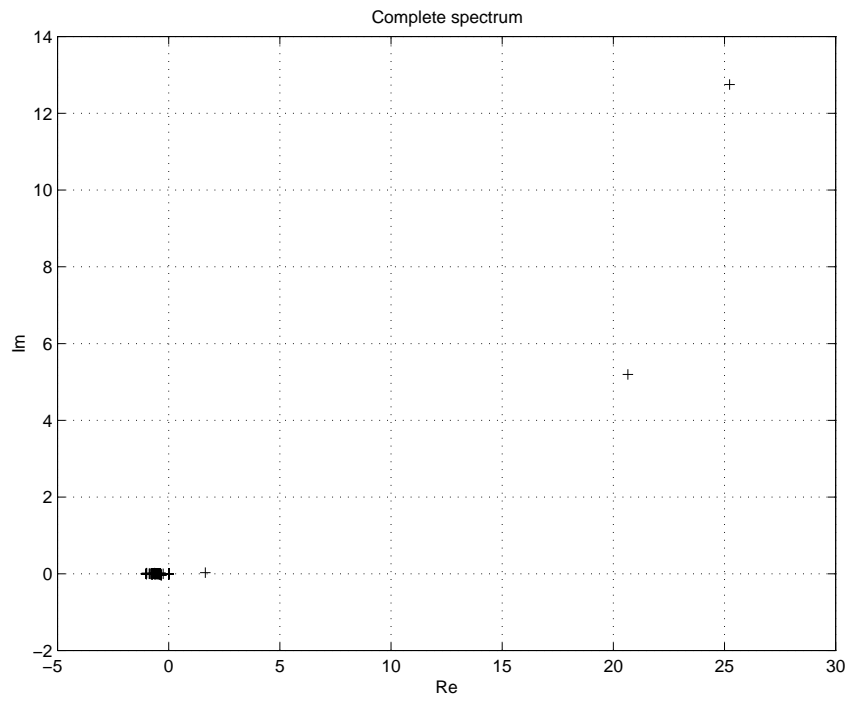
Figures 3 and 4 show one representative case of the spectrum of the iteration operator  $\mathbf{PF}$  from (19) for Neumann boundary condition on the scatterer, and for the elastic scatterer, respectively. The problem setting was as in Section 9, with  $h = 1/40$ ,  $k = 10$ ,  $4 \times 4$  fluid subdomains and, for Figure 4, also  $2 \times 2$  solid subdomains. The coarse space had 4 directions for fluid waves, both for the multipliers and for the wet interface.

The figures show that in both cases, the spectrum is clustered around a point other than the origin. For the coupled problem, there are few more eigenvalues near the origin and some clustered around  $-1$ . The effect of adding the elastic scatterer shows in few extra eigenvalues close to the cluster and a minor change in other eigenvalues.

## 7. IMPLEMENTATION CHOICES

Some implementation details of the algorithms described in Sections 3-5 are slightly different than in FETI-H or were left open and will be specified in this section. The differences are essentially only different choices in implementation. They are not related to the treatment of the coupled problem and do not change the essence of either method, though they of course influence numerical results.

We have generated the matrices  $\mathbf{B}_f$  and  $\mathbf{B}_e$  by creating one equation with coefficients 0, 1,  $-1$  for each pair of subdomains and a degree of freedom they share, in the same way as in FETI, e.g. [27]. To avoid redundant constraints, we have

**FIG. 3.** Spectrum of the FETI-H iteration operator**FIG. 4.** Spectrum of the iteration operator for coupled problem

orthogonalized the rows of the matrices using the QR algorithm. The resulting matrices are still sparse. FETI-H does not orthogonalize the constraint matrices and either leaves redundant constraints in or takes care not to create them.

The columns of the matrix of coarse space generators  $\mathbf{Q}$  from (48) are usually linearly dependent. One reason is aliasing of modes from two subdomains on their interface. Another reason is that the basis of plane waves is ill-conditioned. To obtain a stable numerical algorithm, we have first orthogonalized the columns of  $\mathbf{Y}_f^s$  and  $\mathbf{Y}_e^s$  and then the matrix  $\mathbf{Q}$ , dropping linearly dependent columns in each step. The resulting matrices are still sparse. Since the columns of  $\mathbf{Q}$  are now linearly independent, there is a chance that the coarse system matrix  $\mathbf{Q}^T \mathbf{F} \mathbf{Q}$ , whose decomposition is needed in the coarse coarse correction (20), may be nonsingular. Though this is not guaranteed, the coarse matrices in numerical experiments were always nonsingular. In the case of a singular matrix, one can use a pseudoinverse. FETI-H does not orthogonalize the coarse space generators and deals with the resulting singular coarse matrix by masking zero pivots.

We have used GMRES provided with MATLAB as the iterative solver, while FETI-H uses GCR. The two methods are mathematically equivalent, minimizing the  $\ell^2$  norm of the residual over the Krylov space. GMRES is more complicated and more numerically stable. For more information on Krylov space solvers, see [31].

## 8. COMPLEXITY

To interpret computational results, one needs to estimate the effect of the number of subdomains, subdomain size, and coarse space size on the on the computational complexity of the method. We omit the effect of the orthogonalization of the constraint matrices and coarse space generators on their nonzero structure, and assume that the asymptotic complexity of the algorithm used for the LU decomposition of a block sparse matrix of order  $nm$ , where  $m$  is the order of dense blocks, is proportional to  $n^\alpha m^3$ , and the asymptotic complexity of the multiplication of a vector by the inverse of the LU factors (i.e., the solution) is  $n^\beta m^2$ . For example, for topologically two-dimensional problems and band or profile methods with natural ordering,  $\alpha = 2$  and  $\beta = 1.5$ ; for fully sparse methods, the complexity is less [32]. The complexity the present method is dominated by the LU decomposition of the subdomain matrices, i.e., the diagonal blocks of  $\tilde{\mathbf{A}}_e$  and  $\tilde{\mathbf{A}}_f$ , and the creation and the LU decomposition of the coarse matrix  $\mathbf{Q}^T \mathbf{F} \mathbf{Q}$ .

Denote by  $N$  the total number of degrees of freedom, by  $N_s$  the number of subdomains, by  $N_i$  the total number of degrees of freedom on subdomain interfaces, and by  $N_c$  the number of coarse space basis vectors per subdomain. Assume that all subdomains are about the same size, and there are  $N_t$  interfaces between the subdomains. The number of degrees of freedom per subdomain is  $N/N_s$  on the average.

The total cost of the LU decomposition of the subdomain matrices is about  $N_s(N/N_s)^\alpha$  and the cost of one solution is  $N_s(N/N_s)^\beta$ . We now estimate the cost of creating the first diagonal block of the coarse matrix,  $\mathbf{C} = (\mathbf{D}_f \mathbf{B}_f \mathbf{Y}_f)^T (-\tilde{\mathbf{B}}_f \tilde{\mathbf{A}}_f^{-1} \tilde{\mathbf{B}}_f^T) \mathbf{D}_f \mathbf{B}_f \mathbf{Y}_f$ . This matrix has full blocks which arise by the interaction of  $N_c$  coarse space vectors from two subdomains with a common neighbor, hence it is a topologically  $n$  dimensional block matrix of order asymptotically  $N_s N_c$ , with average block size  $N_c$ . Computing

$(-\tilde{\mathbf{B}}_f \tilde{\mathbf{A}}_f^{-1} \tilde{\mathbf{B}}_f^T) \mathbf{D}_f \mathbf{B}_f \mathbf{Y}_f$  requires  $N_c N_t$  solutions of subdomain problems at  $(N/N_s)^\beta$  each. Multiplication of the result by  $(\mathbf{D}_f \mathbf{B}_f \mathbf{Y}_f)^T$  adds about  $N_c^2 N_s (N_i/N_s)$ . The LU decomposition of  $\mathbf{C}$  costs  $N_s^\alpha N_c^3$  and the solution of a system with  $\mathbf{C}$  costs  $N_s^\beta N_c^2$ . Hence, we get asymptotic estimate of the dominant cost of the setup phase

$$T_{setup} \approx N_s (N/N_s)^\alpha + N_c N_t (N/N_s)^\beta + N_s^\alpha N_c^3 + N_c^2 N_i, \quad (51)$$

and the dominant cost per iteration,

$$T_{iteration} \approx N_s (N/N_s)^\beta + N_s^\beta N_c^2. \quad (52)$$

The estimates for the fluid and elastic subdomains should be done separately following (51), (52) and added together. The complexity of the terms added by the coupling is easily seen to be of lower order. It should be noted that the complexity estimates (51), (52) are not specific to the present method and apply to any nonoverlapping domain decomposition method with a coarse space applied in a similar manner as here, such as the FETI or the Balancing Neumann-Neumann [33] method for positive definite problems.

## 9. COMPUTATIONAL RESULTS

We consider a model 2D problem with a scatterer in the center of a waveguide, cf., Fig. 1. The fluid domain  $\Omega_f$  is a square with side  $1\text{ m}$ , filled with water with density  $\rho_f = 1000\text{ kg m}^{-3}$  and speed of sound  $c_f = 1500\text{ m s}^{-1}$ . The scatterer is a square in the center of the fluid domain, with side  $0.2\text{ m}$  unless specified otherwise in some problems, and consisting of aluminum with density  $\rho_e = 2700\text{ kg m}^{-3}$  and Lamé elasticity coefficients  $\lambda = 5.5263 \cdot 10^{10}\text{ N m}^{-2}$ ,  $\mu = 2.595 \cdot 10^{10}\text{ N m}^{-2}$ .

The fluid domain and the solid domain are discretized by bilinear square elements on a uniform mesh with meshsize  $h$ . Both domains are divided independently into  $m$  by  $n$  subdomains by dividing their horizontal sides into  $m$  intervals of the same length and the vertical sides into  $n$  intervals of the same length, cf., Fig. 2.

In all cases, the constant function is included in the coarse space for the fluid and the rigid body modes are included in the coarse space for the solid, both for the multipliers and for the wet interface.

The stopping criterion for GMRES iterations was  $\|\mathbf{F}\mathbf{x} - \mathbf{b}\| < 10^{-6}$ . The stopping criterion for the iterations does not involve the original variables in the coupled problem (36), which we write here as  $\mathbf{K}\mathbf{z} = \mathbf{d}$ . Since the variables have different scales, and, in addition, the right-hand side in the second block in (36) is zero, the usual relative residual  $\|\mathbf{K}\mathbf{z} - \mathbf{d}\|/\|\mathbf{d}\|$  is meaningless. Instead, we have evaluated the component-wise scaled residual

$$Res = \max_i \frac{|\mathbf{d}_i - \sum_j \mathbf{K}_{ij} \mathbf{z}_j|}{\sum_j |\mathbf{K}_{ij}| |\mathbf{z}_j|}. \quad (53)$$

The numerical results for the model problem are summarized in Tables 1 to 4. The lines in the tables are organized in groups. The first line in the group is the result for the FETI-H method with Neumann condition instead of the elastic scatterer. The following lines are for the elastic scatterer, and they show the number

**TABLE 1**  
**Decreasing  $h$ ,  $k^3 h^2$  constant, constant number of elements per subdomain**

Problem description		Coarse directions				Number of degrees of freedom			Iter.	Res.		
$h$	$k$	Subdomains		$\lambda$		Wet		Orig.			Red.	Crs.
		Fl.	Sol.	Fl.	Sol.	Fl.	Sol.					
1/40	10	2x2	rigid	4				1632	68	11	10	9.2e-07
1/40	10	2x2	1x1	4	0	0	0	1794	140	18	14	3.4e-07
1/40	10	2x2	1x1	4	0	4	0	1794	140	34	11	7.1e-07
1/40	10	2x2	1x1	4	0	4	4	1794	140	35	11	7e-07
1/40	10	2x2	1x1	4	4	4	4	1794	140	35	11	7e-07
1/40	10	2x2	rigid	8				1632	68	18	8	4.9e-07
1/40	10	2x2	1x1	8	0	4	0	1794	140	41	9	5.1e-07
1/40	10	2x2	1x1	8	4	4	4	1794	140	42	9	4.7e-07
1/40	10	2x2	1x1	8	4	8	8	1794	140	58	9	3e-07
1/40	10	2x2	1x1	8	8	8	8	1794	140	58	9	3e-07
1/80	16	4x4	rigid	4				6336	464	63	15	4.5e-07
1/80	16	4x4	2x2	4	0	0	0	6914	674	84	25	7.6e-07
1/80	16	4x4	2x2	4	0	4	0	6914	674	100	24	5.7e-07
1/80	16	4x4	2x2	4	0	4	4	6914	674	102	24	5.8e-07
1/80	16	4x4	2x2	4	4	4	4	6914	674	111	21	1.3e-06
1/80	16	4x4	rigid	8				6336	464	102	11	6e-07
1/80	16	4x4	2x2	8	0	4	0	6914	674	139	21	6.8e-07
1/80	16	4x4	2x2	8	4	4	4	6914	674	150	18	8.8e-07
1/80	16	4x4	2x2	8	4	8	8	6914	674	172	18	8.4e-07
1/80	16	4x4	2x2	8	8	8	8	6914	674	183	13	1.2e-06
1/160	25	8x8	rigid	4				24960	2240	287	17	1.6e-06
1/160	25	8x8	4x4	4	0	0	0	27138	2930	352	55	7.5e-07
1/160	25	8x8	4x4	4	0	4	0	27138	2930	368	43	1.3e-06
1/160	25	8x8	4x4	4	0	4	4	27138	2930	378	43	1.2e-06
1/160	25	8x8	4x4	4	4	4	4	27138	2930	426	40	7e-07
1/160	25	8x8	rigid	8				24960	2240	462	16	4.4e-07
1/160	25	8x8	4x4	8	0	4	0	27138	2930	543	33	1.3e-06
1/160	25	8x8	4x4	8	4	4	4	27138	2930	601	31	1.1e-06
1/160	25	8x8	4x4	8	4	8	8	27138	2930	635	30	1.3e-06
1/160	25	8x8	4x4	8	8	8	8	27138	2930	695	20	1.7e-06

**TABLE 2**  
**Decreasing  $h$ ,  $k^3h^2$  constant, same subdomains**

Problem description				Coarse directions				Number of degrees of freedom			Iter.	Res.
$h$	$k$	Subdomains		$\lambda$		Wet		Orig.	Red.	Crs.		
		Fl.	Sol.	Fl.	Sol.	Fl.	Sol.					
1/40	10	4x4	rigid	4				1632	240	63	11	7.3e-07
1/40	10	4x4	2x2	4	0	0	0	1794	354	84	18	3.7e-07
1/40	10	4x4	2x2	4	0	4	0	1794	354	100	16	1.1e-06
1/40	10	4x4	2x2	4	0	4	4	1794	354	104	16	1.2e-06
1/40	10	4x4	2x2	4	4	4	4	1794	354	112	15	3.7e-07
1/40	10	4x4	rigid	8				1632	240	102	7	5.4e-07
1/40	10	4x4	2x2	8	0	4	0	1794	354	139	13	5e-07
1/40	10	4x4	2x2	8	4	4	4	1794	354	151	11	7e-07
1/40	10	4x4	2x2	8	4	8	8	1794	354	175	11	6.5e-07
1/40	10	4x4	2x2	8	8	8	8	1794	354	187	7	1.2e-06
1/80	16	4x4	rigid	4				6336	464	63	15	4.5e-07
1/80	16	4x4	2x2	4	0	0	0	6914	674	84	25	7.6e-07
1/80	16	4x4	2x2	4	0	4	0	6914	674	100	24	5.7e-07
1/80	16	4x4	2x2	4	0	4	4	6914	674	102	24	5.8e-07
1/80	16	4x4	2x2	4	4	4	4	6914	674	111	21	1.3e-06
1/80	16	4x4	rigid	8				6336	464	102	11	6e-07
1/80	16	4x4	2x2	8	0	4	0	6914	674	139	21	6.8e-07
1/80	16	4x4	2x2	8	4	4	4	6914	674	150	18	8.8e-07
1/80	16	4x4	2x2	8	4	8	8	6914	674	172	18	8.4e-07
1/80	16	4x4	2x2	8	8	8	8	6914	674	183	13	1.2e-06
1/160	25	4x4	rigid	4				24960	912	63	28	1.5e-06
1/160	25	4x4	2x2	4	0	0	0	27138	1314	84	50	1.1e-06
1/160	25	4x4	2x2	4	0	4	0	27138	1314	100	43	5.2e-07
1/160	25	4x4	2x2	4	0	4	4	27138	1314	101	42	1.4e-06
1/160	25	4x4	2x2	4	4	4	4	27138	1314	109	39	1e-06
1/160	25	4x4	rigid	8				24960	912	102	17	7.7e-07
1/160	25	4x4	2x2	8	0	4	0	27138	1314	139	35	5.7e-07
1/160	25	4x4	2x2	8	4	4	4	27138	1314	148	30	1.4e-06
1/160	25	4x4	2x2	8	4	8	8	27138	1314	171	28	1.5e-06
1/160	25	4x4	2x2	8	8	8	8	27138	1314	181	24	1.2e-06
1/320	40	4x4	rigid	4				99072	1808	63	56	1.8e-06
1/320	40	4x4	2x2	4	0	0	0	107522	2594	84	87	8.9e-07
1/320	40	4x4	2x2	4	0	4	0	107522	2594	100	79	4.2e-07
1/320	40	4x4	2x2	4	0	4	4	107522	2594	100	79	4.2e-07
1/320	40	4x4	2x2	4	4	4	4	107522	2594	108	73	8e-07
1/320	40	4x4	rigid	8				99072	1808	102	24	1.5e-06
1/320	40	4x4	2x2	8	0	4	0	107522	2594	139	48	5.4e-07
1/320	40	4x4	2x2	8	4	4	4	107522	2594	147	43	5e-07
1/320	40	4x4	2x2	8	4	8	8	107522	2594	171	40	7.7e-07
1/320	40	4x4	2x2	8	8	8	8	107522	2594	183	34	5.3e-07

TABLE 3

Increasing the number of fluid and elastic subdomains, obstacle size 0.5

Problem description				Coarse directions				Number of degrees of freedom			Iter.	Res.
$h$	$k$	Subdomains		$\lambda$		Wet		Orig.	Red.	Crs.		
		Fl.	Sol.	Fl.	Sol.	Fl.	Sol.					
1/200	80	2x2	rigid	4				30600	204	11	29	1.2e-06
1/200	80	2x2	2x2	4	0	0	0	51002	1422	32	128	8.7e-07
1/200	80	2x2	2x2	4	0	4	0	51002	1422	48	125	7.1e-07
1/200	80	2x2	2x2	4	0	4	4	51002	1422	48	125	7.1e-07
1/200	80	2x2	2x2	4	4	4	4	51002	1422	56	117	6.4e-07
1/200	80	2x2	rigid	8				30600	204	18	22	7.5e-07
1/200	80	2x2	2x2	8	0	4	0	51002	1422	55	117	5.4e-07
1/200	80	2x2	2x2	8	4	4	4	51002	1422	63	108	6.2e-07
1/200	80	2x2	2x2	8	4	8	8	51002	1422	87	99	7e-07
1/200	80	2x2	2x2	8	8	8	8	51002	1422	99	86	6.9e-07
1/200	80	4x4	rigid	4				30600	612	36	73	2.2e-07
1/200	80	4x4	4x4	4	0	0	0	51002	2666	105	no convergence	
1/200	80	4x4	4x4	4	0	4	0	51002	2666	121	no convergence	
1/200	80	4x4	4x4	4	0	4	4	51002	2666	132	no convergence	
1/200	80	4x4	4x4	4	4	4	4	51002	2666	180	192	7.6e-07
1/200	80	4x4	rigid	8				30600	612	60	49	2.6e-07
1/200	80	4x4	4x4	8	0	4	0	51002	2666	145	200	3.9e-06
1/200	80	4x4	4x4	8	4	4	4	51002	2666	204	163	6.8e-07
1/200	80	4x4	4x4	8	4	8	8	51002	2666	237	146	7.7e-07
1/200	80	4x4	4x4	8	8	8	8	51002	2666	297	107	1e-06

TABLE 4

Increasing the number of elastic subdomains, obstacle size 0.9

Problem description				Coarse directions				Number of degrees of freedom			Iter.	Res.
$h$	$k$	Subdomains		$\lambda$		Wet		Orig.	Red.	Crs.		
		Fl.	Sol.	Fl.	Sol.	Fl.	Sol.					
1/200	32	2x2	rigid	4				8360	44	11	7	1e-06
1/200	32	2x2	2x2	4	0	0	0	73882	2222	32	99	4.4e-07
1/200	32	2x2	2x2	4	0	4	0	73882	2222	48	93	6.9e-07
1/200	32	2x2	2x2	4	0	4	4	73882	2222	48	93	6.9e-07
1/200	32	2x2	2x2	4	4	4	4	73882	2222	56	87	5.8e-07
1/200	32	2x2	rigid	8				8360	44	18	6	1.7e-07
1/200	32	2x2	2x2	8	0	4	0	73882	2222	55	92	5.6e-07
1/200	32	2x2	2x2	8	4	4	4	73882	2222	63	85	5.7e-07
1/200	32	2x2	2x2	8	4	8	8	73882	2222	87	66	1.3e-06
1/200	32	2x2	2x2	8	8	8	8	73882	2222	99	55	1e-06
1/200	32	2x2	rigid	4				8360	44	11	7	1e-06
1/200	32	2x2	4x4	4	0	0	0	73882	3694	76	137	4e-07
1/200	32	2x2	4x4	4	0	4	0	73882	3694	92	128	5.8e-07
1/200	32	2x2	4x4	4	0	4	4	73882	3694	107	126	7.2e-07
1/200	32	2x2	4x4	4	4	4	4	73882	3694	155	101	9.4e-07
1/200	32	2x2	rigid	8				8360	44	18	6	1.7e-07
1/200	32	2x2	4x4	8	0	4	0	73882	3694	99	126	5.4e-07
1/200	32	2x2	4x4	8	4	4	4	73882	3694	162	99	9.6e-07
1/200	32	2x2	4x4	8	4	8	8	73882	3694	187	76	8.9e-07
1/200	32	2x2	4x4	8	8	8	8	73882	3694	247	45	9.4e-07

of iterations for increasing the number of coarse space functions, that is, the columns of  $\mathbf{Q}$ . The headings in the tables are:

1.  $1/h$  - the mesh spacing
2.  $k$  - the wave number
3. Subdomains Fl. - the number of fluid subdomains
4. Subdomain Sol. - the number of elastic subdomains, or “rigid” if only the Helmholtz equation in the fluid is solved
5. Coarse directions  $\lambda$  Fl. - the number of directions per fluid subdomain of plane waves for multipliers in the coarse problem
6. Coarse directions  $\lambda$  Sol. - the number of directions per elastic subdomain of plane pressure and shear waves and plane shear waves for multipliers in the coarse problem
7. Coarse directions Wet Fl. - the number of directions per fluid subdomain of plane waves for the wet interface in the coarse problem
8. Coarse directions Wet Sol. - the number of directions per elastic subdomain of plane pressure and shear waves for the wet interface in the coarse problem
9. Number of degrees of freedom Orig. - the size of the algebraic problem solved
10. Number of degrees of freedom Red. - the number of degrees of freedom in the reduced problem, i.e., the order of the matrix  $\mathbf{F}$
11. Number of degrees of freedom Crs. - the size of the coarse problem after orthogonalization of the coarse space generators
12. Iter. - the number of iterations
13. Res. - the component-wise scaled residual of the coupled problem from (53)

The scaled residual (53) was of the same order of magnitude as the tolerance in the stopping criterion or smaller.

The results in Tables 1 and 2 show scalability when the mesh is refined and the frequency increased while keeping  $k^3 h^2$  constant, which is needed to avoid pollution by the phase error and to keep the error decreasing with  $h$  for the Helmholtz equation, cf., Ihlenburg and Babuška [34]. We first keep the number of elements per subdomain constant and then we keep the number of subdomains constant. Tables 3 and 4 show convergence for increasing the number of elastic subdomains. Because we want to isolate the effect of the elastic domain, the obstacle is made larger. The fluid domain is smaller (in the test problems in Table 4, the fluid domain consists of just few layers of elements), so the number of iterations for the rigid case is much lower.

Clearly, increasing the size of the coarse space decreases the number of iterations. The prototype implementation was done in MATLAB, hence we do not report timings. However, we should note that the most time-consuming operation was the generation of the data and assembling the subdomain matrices, followed by the setup of the iterative method, and the iterations themselves were only a small fraction of the overall time (when the method converged).

## 10. CONCLUSION

We have presented a new iterative substructuring method for coupled fluid-solid scattering problems. The computational results indicate that the method is scalable

with respect to mesh size, frequency, and the number of subdomains. The growth of the number of iterations can be controlled by increasing the size of the coarse space. Numerical calculation of the spectrum of the iteration operator suggests that the fast convergence is due to clustering of the spectrum. In most cases, the resulting number of iterations is same or slightly larger than for the FETI-H method for the same problem with the Neumann boundary condition instead of an elastic scatterer.

### ACKNOWLEDGMENT

This research was supported in part by the Office of Naval Research under grant N-00014-95-1-0663, and the National Science foundation under grants ECS-9725504 and DMS-007428. The author would like to thank Charbel Farhat, Rabia Djellouli, and other coworkers at the Center for Aerospace Structures at the University of Colorado at Boulder for useful discussions, stimulating remarks, and their patience during several presentations of early versions of this work, and to anonymous referees for their helpful comments. The prototype MATLAB code used parts of a code originally written by Mirela Popa and the author [35].

### REFERENCES

1. A. I. Achil'diev and Kh. S. Nazhmidinov. An iterative method for solving a diffraction problem in an unbounded medium. *Dokl. Akad. Nauk Tadzhik. SSR*, 31(7):429–432, 1988. In Russian.
2. Peter Cummings and Xiaobing Feng. Domain decomposition methods for a system of coupled acoustic and elastic Helmholtz equations. In *Eleventh International Conference on Domain Decomposition Methods (London, 1998)*, pages 206–213 (electronic). DDM.org, Augsburg, 1999.
3. A. De La Bourdonnaye, C. Farhat, A. Macedo, F. Magoulès, and F.-X. Roux. A non-overlapping domain decomposition method for the exterior Helmholtz problem. *Contemporary Mathematics*, 218:42–66, 1998. Proceedings of the Tenth Conference on Domain Decomposition, J. Mandel, C. Farhat, and X.-C. Cai, eds.
4. C. Farhat, A. Macedo, M. Lesoinne, F.-X. Roux, F. Magoulès, and A. De La Bourdonnaye. Two-level domain decomposition methods with Lagrange multipliers for the fast solution of acoustic scattering problems. *Comput. Methods Appl. Mech. Engrg.*, 184(2-4):213–239, 2000.
5. C. Farhat, A. Macedo, and R. Tezaur. FETI-H: a scalable domain decomposition method for high frequency exterior Helmholtz problems. In Choi-Hong Lai, Petter Børstø, Mark Cross, and Olof Widlund, editors, *Eleventh International Conference on Domain Decomposition Method*, pages 231–241. DDM.ORG, 1999.
6. Charbel Farhat and Francois-Xavier Roux. An unconventional domain decomposition method for an efficient parallel solution of large-scale finite element systems. *SIAM J. Sci. Stat. Comput.*, 13:379–396, 1992.
7. Charbel Farhat, Jan Mandel, and Francois-Xavier Roux. Optimal convergence properties of the FETI domain decomposition method. *Comput. Methods Appl. Mech. Engrg.*, 115:367–388, 1994.
8. Jan Mandel and Radek Tezaur. Convergence of a substructuring method with Lagrange multipliers. *Numerische Mathematik*, 73:473–487, 1996.
9. Charbel Farhat and Jan Mandel. The two-level FETI method for static and dynamic plate problems - Part I: An optimal iterative solver for biharmonic systems. *Comp. Meth. Appl. Mech. Engrg.*, 155:129–152, 1998.
10. Charbel Farhat and Jan Mandel. Scalable substructuring by Lagrange multipliers in theory and practice. In *Proceedings of the 9th International Conference on Domain Decomposition, Bergen, Norway, June 1996*, pages 20–30. DDM.ORG, 1998.
11. Axel Klawonn and Olof B. Widlund. A domain decomposition method with Lagrange multipliers and inexact solvers for linear elasticity. *SIAM J. Sci. Comput.*, 22(4):1199–1219, October 2000.
12. Axel Klawonn and Olof B. Widlund. FETI and Neumann-Neumann iterative substructuring methods: Connections and new results. *Comm. Pure Appl. Math.*, 54:57–90, January 2001.

13. Jan Mandel, Radek Tezaur, and Charbel Farhat. A scalable substructuring method by Lagrange multipliers for plate bending problems. *SIAM J. Numer. Anal.*, 36:1370–1391, 1999.
14. K. C. Park, M. R. Justino, Jr., and C. A. Felippa. An algebraically partitioned FETI method for parallel structural analysis: Algorithm description. *Int. J. Numer. Meth. Engrg.*, 40:2717–2737, 1997.
15. Daniel J. Rixen, Charbel Farhat, Radek Tezaur, and Jan Mandel. Theoretical comparison of the FETI and algebraically partitioned FETI methods, and performance comparisons with a direct sparse solver. *Int. J. Numer. Meth. Engrg.*, 46:501–534, 1999.
16. Bruno Després. Domain decomposition method and the Helmholtz problem. In Gary Cohen, Laurence Halpern, and Patrick Joly, editors, *Mathematical and numerical aspects of wave propagation phenomena (Strasbourg, 1991)*, pages 44–52. SIAM, Philadelphia, PA, 1991.
17. Lynn Schreyer Bennethum and Xiaobing Feng. A domain decomposition method for solving a Helmholtz-like problem in elasticity based on the Wilson nonconforming element. *RAIRO Modél. Math. Anal. Numér.*, 31(1):1–25, 1997.
18. C. Farhat, A. Macedo, and M. Lesoinne. A two-level domain decomposition method for the iterative solution of high frequency exterior Helmholtz problem. *Numerische Mathematik*, 85:283–308, 2000.
19. Radek Tezaur, Antonini Macedo, and Charbel Farhat. Iterative solution of large-scale acoustic scattering problems with multiple right hand-sides by a domain decomposition method with Lagrange multipliers. *Internat. J. Numer. Methods Engrg.*, 51(10):1175–1193, 2001.
20. Manish Malhotra, Roland W. Freund, and Peter M. Pinsky. Iterative solution of multiple radiation and scattering problems in structural acoustics using a block quasi-minimal residual algorithm. *Comput. Methods Appl. Mech. Engrg.*, 146(1-2):173–196, 1997.
21. Assad A. Oberai, Manish Malhotra, and Peter M. Pinsky. On the implementation of the Dirichlet-to-Neumann radiation condition for iterative solution of the Helmholtz equation. *Appl. Numer. Math.*, 27(4):443–464, 1998.
22. Charles I. Goldstein. Multigrid preconditioners applied to the iterative solution of singularly perturbed elliptic boundary value problems and scattering problems. In R.P. Shaw, J. Periaux, A. Chaudouet, J. Wu, C. Marino, and C.A. Brebbia, editors, *Innovative numerical methods in engineering, Proc. 4th Int. Symp., Atlanta/Ga., 1986*, pages 97–102, Berlin, 1986. Springer-Verlag.
23. B. Lee, T. A. Manteuffel, S. F. McCormick, and J. Ruge. First-order system least-squares for the Helmholtz equation. *SIAM J. Sci. Comput.*, 21(5):1927–1949 (electronic), 2000. Iterative methods for solving systems of algebraic equations (Copper Mountain, CO, 1998).
24. Petr Vaněk, Jan Mandel, and Marian Brezina. Two-level algebraic multigrid for the Helmholtz problem. In J. Mandel, C. Farhat, and X.-C. Cai, editors, *Tenth International Conference on Domain Decomposition*, volume 218 of *Contemporary Mathematics*, pages 349–356, Providence, RI, 1998. American Mathematical Society.
25. Charbel Farhat, Michel Lesoinne, Patrick LeTallec, Kendall Pierson, and Daniel Rixen. FETI-DP: a dual-primal unified FETI method. I. A faster alternative to the two-level FETI method. *Internat. J. Numer. Methods Engrg.*, 50(7):1523–1544, 2001.
26. Jan Mandel and Radek Tezaur. On the convergence of a dual-primal substructuring method. *Numerische Mathematik*, 88:543–558, 2001.
27. Charbel Farhat and Francois-Xavier Roux. Implicit parallel processing in structural mechanics. *Comput. Mech. Advances*, 2:1–124, 1994.
28. J. L. Lions. Contribution à un problème de M. M. Picone. *Ann. Mat. Pura Appl. (4)*, 41:201–219, 1956.
29. V.K. Varadan and V.V. Varadan. Acoustic, electromagnetic, and elastodynamic fields. In V.K. Varadan and V.V. Varadan, editors, *Field Representations and Introduction to Scattering*. North-Holland, Amsterdam, 1991.
30. Henri J.-P. Morand and Roger Ohayon. *Fluid Structure Interaction*. John Wiley and Sons, Chichester, 1995.
31. Anne Greenbaum. *Iterative Methods for Solving Linear Systems*. SIAM, Philadelphia, 1997.
32. I. S. Duff, A. M. Erisman, and J. K. Reid. *Direct Methods for Sparse Matrices*. Clarendon Press, Oxford, 1986.

33. Jan Mandel. Balancing domain decomposition. *Comm. in Numerical Methods in Engrg.*, 9:233–241, 1993.
34. F. Ihlenburg and I. Babuška. Finite element solution of the Helmholtz equation with high wave number. I. The  $h$ -version of the FEM. *Comput. Math. Appl.*, 30(9):9–37, 1995.
35. Jan Mandel and Mirela Popa. A multigrid method for elastic scattering. UCD/CCM Report 109, Center for Computational Mathematics, University of Colorado at Denver, September 1997. <http://www-math.cudenver.edu/ccmreports/rep109.ps.gz>.